Available online at www.sciencedirect.com
ScienceDirect
Journal of Sound and Vibration 299 (2007) 854–868
JOURNAL OF SOUND AND VIBRATION
www.elsevier.com/locate/jsvi

Moderately large vibrations of doubly curved shallow open shells composed of thick layers

Christoph Adam*

Leopold-Franzens-University of Innsbruck, Technikerstr. 13, 6020 Innsbruck, Austria

Received 21 March 2005; received in revised form 2 May 2006; accepted 19 July 2006
Available online 24 October 2006

Abstract

This paper addresses nonlinear flexural vibrations of shallow shells composed of three thick layers with different shear flexibility, which are symmetrically arranged with respect to the middle surface. The considered shell structures of polygonal planform are hard hinged simply supported (i.e. all in-plane rotations and the bending moment vanish) with the edges fully restraint against displacements in any direction. The kinematic field equations are formulated by layerwise application of a first-order shear deformation theory. A modification of Berger's theory is employed to model the nonlinear characteristics of the structural response. The continuity of the transverse shear stress across the interfaces is specified according to Hooke's law, and subsequently the equations of motion of this higher order problem can be derived in analogy to a homogeneous single-layer shear deformable shallow shell. Numerical results of rectangular shallow shells in nonlinear steady-state vibration are presented for various ratios of shell rise to thickness, and non-dimensional load amplitude.
© 2006 Elsevier Ltd. All rights reserved.

1. Introduction

Shells are three-dimensional structural elements bounded by two relatively closely spaced curved surfaces, which are frequently employed in various civil, mechanical, and aeronautical engineering applications. Because of their practical importance various shell theories have been developed in order to predict accurately the static and dynamic response to mechanical loadings for preliminary design analyses. These theories cover thin and thick shell theories, shallow and deep theories, linear and nonlinear theories among others. Comprehensive surveys of Qatu [1,2] and Alhazza and Alhazza [3] provide insight into several shell theories and their limitations.

In the present study the focus is on doubly curved open shallow shells composed of three thick layers of different shear flexibility. It is noted that shallow shells refer to shells with a rise of no more than $\frac{1}{5}$ the smallest planform dimension [1]. Although their particular importance is widely recognized, the number of research papers devoted to moderately large vibrations of this class of layered shallow shells, where a layerwise formulation of the kinematic field equations is required, is relatively small. This observation is supported by

*Corresponding author. Tel.: +43 512 507 6585; fax: +43 512 507 2908.
E-mail address: christoph.adam@uibk.ac.at.

0022-460X/$ - see front matter © 2006 Elsevier Ltd. All rights reserved.
doi:10.1016/j.jsv.2006.07.044

review papers concerning shallow shells of Liew et al. [4] and Qatu [1]. Examples of contributions in the field of nonlinear structural vibration analysis of layered (shallow) shells can be found in Ref. [5–11]. However, it may be of significance for some implementations to describe more precisely the effects of layerwise different transverse shear flexibility in combination with nonlinear response issues.

In this paper, based upon a layerwise first-order shear deformation theory, the governing equations for moderately large vibrations of doubly curved layered shallow shells with polygonal planform are derived, expanding the ideas sketched for composite plates in Ref. [12]. Material properties and geometry of the layers are symmetrically arranged about the middle surface. The boundaries of the considered shell structures are hard hinged simply supported (i.e., all in-plane rotations are restrained, and the bending moment is zero) with the displacements in all directions fully restrained. In the mechanical model the nonlinear response generated by moderately large vibration amplitudes is considered via Berger's theory [13] modified by a layerwise application of the Mindlin–Reissner kinematic hypothesis. Results of rectangular shaped shells are presented in form of amplitude frequency response functions, and they demonstrate the effects of interactions between the initial curvature, transverse shear flexibility, and time-harmonic mechanical loads on the hardening and/or softening type of the nonlinear response.

2. Basic equations

In the present analysis, an open doubly curved shallow shell composed of three thick isotropic layers is considered. The layers are perfectly bonded, and thickness and linear elastic properties of the upper and lower face are symmetrically arranged with respect to the middle surface. Faces and core may exhibit extremely different elastic moduli with a common Poisson's ratio ν. The shell is referred to the curvilinear coordinates x and y that follow the lines of principal curvature, and z is a coordinate outward perpendicular to the curved middle surface (see Fig. 1). The edges of the shallow shell with polygonal planform are hard hinged supported and the displacements normal to the edge face are fully restrained (i.e., along the edge the displacements in all directions and the in-plane rotations are restrained, and the bending moment is zero). The contour of the middle surface and its projected plane (in Fig. 1 denoted by xy-plane) coincide, i.e. all edges are straight. Throughout the paper index $i = 2$ refers to quantities of the core, whereas $i = 1, 3$ belong to the lower and upper face, respectively (Fig. 2).

Let $k_x = R^{-1}{}_x$ and $k_y = R^{-1}{}_y$ denote the principal curvatures, and ${}_2u_x^{(0)}$, ${}_2u_y^{(0)}$, w the components of the displacement at the middle surface in x, y and z direction, respectively. Applying a first-order shear deformation theory to each thick layer separately the in-plane displacements ${}_iu_x$, ${}_iu_y$ in the ith layer in x and y direction, respectively, at distance z from the middle surface may be expressed as [15]

$$ {}_iu_j(x,y,z) = {}_iu_j^0(x,y,z) + z\,{}_i\psi_j(x,y), \quad i = 1,2,3, \quad j = x,y. \tag{1} $$

${}_iu_x^{(0)}$, ${}_iu_y^{(0)}$ denote in-plane displacements at $z = 0$ (see Fig. 2), and ${}_i\psi_x$, ${}_i\psi_y$ are layerwise cross-sectional rotations, $i = 1, 2, 3$.

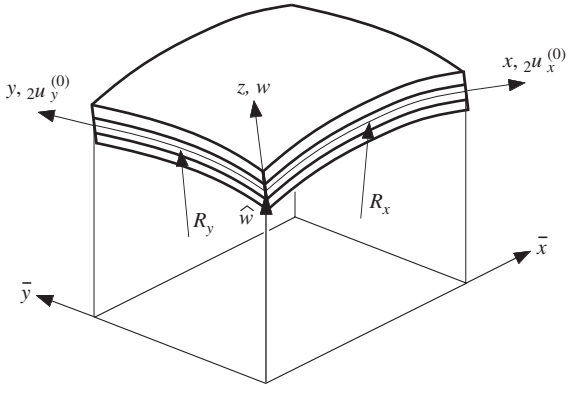

Fig. 1. Geometry and coordinate system of a three-layer shallow shell element.

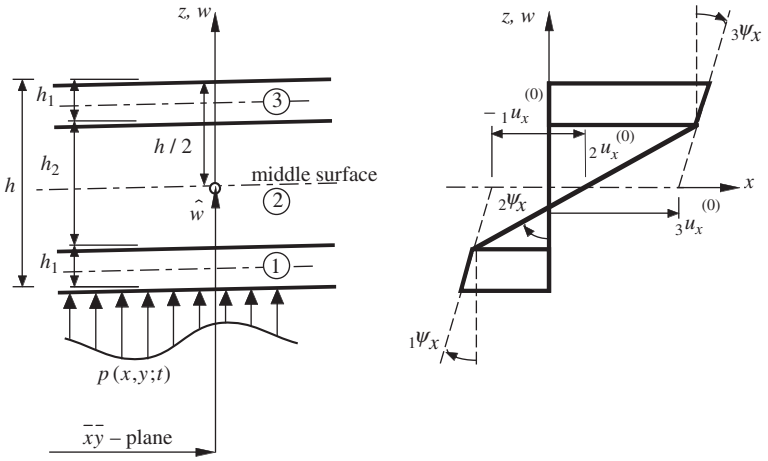

Fig. 2. Three-layer composite shallow shell, xz-plane. Corresponding horizontal displacement field.

Assuming perfect bond between the layers (i.e. no interlayer slip is admitted), the in-plane displacements ${}_iu_x^{(0)}$, ${}_iu_y^{(0)}$ of the faces ($i = 1, 3$) can be expressed in terms of the in-plane displacements of the middle surface ${}_2u_x^{(0)}$, ${}_2u_y^{(0)}$ and the cross-sectional rotations (see Fig. 2) [12]:

$$ {}_iu_j^{(0)}(x,y) = {}_2u_j^{(0)}(x,y) + z_i\left[{}_2\psi_j(x,y) - {}_i\psi_j(x,y)\right], \quad i = 1,3, \quad j = x,y, \tag{2} $$

where $z_1 = -h_2/2$, $z_3 = h_2/2$ denote normal distances from the middle surface to the upper and lower interface, respectively.

Moderately large deflections w lead to an interaction between the membrane stresses and the curvatures, which is reflected by nonlinear terms in the strain–displacement relations. According to von Kármán and Tsien [14] the nonlinear middle surface strains for moderately large deflections w are given by:

$$ e_j(x,y) = {}_2u_{j,j}^{(0)}(x,y) + w(x,y)k_j(x,y) + \tfrac{1}{2}\left[w_{,j}(x,y)\right]^2, \quad j = x,y, \tag{3a} $$

$$ e_{xj}(x,y) = {}_2u_{x,y}^{(0)}(x,y) + {}_2u_{y,x}^{(0)}(x,y) + w_{,x}(x,y)w_{,y}(x,y). \tag{3b} $$

Comma denotes partial differentiation with respect the corresponding coordinates x and y. The strains at distance z from the middle surface become:

$$ {}_i\varepsilon_j(x,y,z) = {}_iu_{j,j}(x,y,z) + w(x,y)k_j(x,y) + \tfrac{1}{2}\left[w_{,j}(x,y)\right]^2, \tag{4a} $$

$$ \begin{aligned} {}_i\gamma_{xy}(x,y,z) &= {}_iu_{x,y}(x,y,z) + {}_iu_{y,x}(x,y,z) + w_{,x}(x,y)w_{,y}(x,y), \\ {}_i\gamma_{jz}(x,y,z) &= {}_iu_{j,z}(x,y,z) + w_j(x,y), \quad i = 1,2,3, \quad j = x,y. \end{aligned} \tag{4b} $$

The constitutive relations are linear. For an isotropic, elastic material the stress components σ_x, σ_y, τ_{xy} are related to the strains by means of the Hooke's law, see e.g., Ref. [16],

$$ {}_i\sigma_j = \frac{2G_i}{1-\nu}\left({}_i\varepsilon_j + \nu\ {}_i\varepsilon_k\right), \quad {}_i\tau_{xy} = G_i\ {}_i\gamma_{xy}, \quad i = 1,2,3, \quad j = x, \quad k = y \quad \text{and} \quad j = y, \quad k = x, \tag{5} $$

where G_i is the shear modulus of the isotropic ith layer. The normal stress component σ_z is assumed to be negligible and subsequently dropped.

Transverse shear stress components τ_{xz}, τ_{yz} are specified to be continuous across the interfaces. Two types of approximations are acknowledged in the literature. The "correct" shear stress expressed by means of the law of conservation of momentum satisfies the in-plane equilibrium by itself, see e.g., Ref. [15]. Alternatively, prescribing the continuity of the transverse shear stresses according to Hooke's law renders a simplified boundary value problem [17–19],

$$ {}_i\tau_{jz} = G_i\Big({}_i\psi_j + w_{,j}\Big), \quad {}_{i+1}\tau_{jz} = G_{i+1}\Big({}_{i+1}\psi_j + w_{,j}\Big), \quad i = 1,2, \quad j = x,y, \tag{6} $$

In analogy to the Mindlin theory for homogeneous plates, Eq. (6) exhibits the simplified assumption that the shear stress is uniformly distributed throughout the layers. From this relation and in combination with $G_1 = G_3$ it follows that the cross-sectional rotations of both faces are identical,

$$ {}_1\psi_j = {}_3\psi_j, \quad j = x,y. \tag{7} $$

Layerwise stress resultants, i.e., the layerwise moment resultants ${}_im_x$, ${}_im_y$, ${}_im_{xy}$ and shear force resultants ${}_iq_x$, ${}_iq_y$ are determined by integration of the stress components, Eq. (5), with respect to the thickness of the layers,

$$ {}_im_j = \int_{a_i}^{a_{i+1}} {}_i\sigma_j z\,\mathrm{d}z, \quad {}_im_{xy} = \int_{a_i}^{a_{i+1}} {}_i\tau_{xy} z\,\mathrm{d}z, \quad {}_iq_j = \int_{a_i}^{a_{i+1}} {}_i\tau_{xy}\,\mathrm{d}z, \quad i = 1,2,3, \quad j = x,y. \tag{8} $$

Utilizing Eqs. (6) and (7) the cross-sectional rotations of the faces are eliminated, and hence, the layerwise resultants can be expressed in terms of the lateral deflection w, the cross-sectional rotations ${}_2\psi_x$, ${}_2\psi_y$ of the core, the middle surface strains and their derivatives.

The overall stress resultants of the shallow shell are determined by layerwise summation,

$$ m_j = \sum_{i=1}^{3} {}_im_j, \quad m_{xy} = \sum_{i=1}^{3} {}_im_{xy}, \quad q_j = \sum_{i=1}^{3} {}_iq_j, \quad j = x,y \tag{9} $$

and they are obtained as (see also Ref. [12]),

$$ m_j = \frac{2}{1-\nu}\sum_{i=1}^{3}\Big\{(\beta_i + C_i){}_2\psi_{j,j} + \beta_i w_{,jj} + \nu\big[(\beta_i + C_i){}_2\psi_{k,k} + \beta_i w_{,kk}\big]\Big\}, $$
$$ j = x, \ k = y \quad \text{and} \quad k = x, \ j = y, \tag{10a} $$

$$ m_{xy} = \sum_{i=1}^{3}\Big[(\beta_i + C_i)\Big({}_2\psi_{x,y} + {}_2\psi_{y,x}\Big) + 2\beta_i w_{,xy}\Big], \tag{10b} $$

$$ q_j = \frac{1}{\chi}\Big({}_2\psi_j + w_{,j}\Big), \quad j = x,y. \tag{11} $$

A_i, B_i and C_i represent layerwise stiffness coefficients:

$$ A_i = G_i h_i, \ \ B_i = \tfrac{1}{2}G_i\big(a_{i+1}^2 - a_i^2\big), \ \ C_i = \tfrac{1}{3}G_i\big(a_{i+1}^3 - a_i^3\big), \quad i = 1,2,3, \tag{12a} $$

$$ a_1 = -h/2, \ \ a_2 = -h_2/2, \ \ a_3 = h_2/2, \ \ a_4 = h_2/2, \tag{12b} $$

χ denotes an overall shear rigidity and s_i are layerwise shear rigidities,

$$ \chi = \frac{s_1 s_2 G_1}{2s_2 G_2 + s_1 G_1}, \ \ s_1 = \frac{1}{\kappa^2 G_i h_i}, \quad i = 1,2,3, \tag{13} $$

and

$$ \beta_1 = \beta_3 = \left(\frac{1}{2}B_1 h_2 + C_1\right)\left(\frac{G_2}{G_1} - 1\right), \ \ \beta_2 = 0. \tag{14} $$

In Eq. (13), a shear correction factor κ^2 is employed, because the transverse shear stresses are assumed to be constant through the thickness. This is the same concept used in the Mindlin–Reissner theories for thick plates. The proper choice of κ^2 is discussed in Ref. [15].

The in-plane displacements of the middle surface at the edges Γ are fully restrained, i.e. ${}_2u_x^{(0)}|_\Gamma = 0$, ${}_2u_y^{(0)}|_\Gamma = 0$, and hence, according to Nash and Modeer [20] moderately large lateral deflections of shallow shells may be considered simplified by means of Berger's approximation. This approximation is based on the assumption that the elastic energy given by the second invariant of the middle surface strain

tensor may be disregarded as compared to the square of the first invariant without substantially affecting the response. In Berger's approach, the influence of the in-plane force resultants is characterized by a time-dependent isotropic force n, which is a constant throughout the shell domain Ω, compare [8,21],

$$n = -\frac{D}{2\Omega}\int_{\Omega} w(\Delta w - 4H)\,\mathrm{d}\Omega, \tag{15}$$

where

$$D = \frac{2}{1-\nu}\sum_{i=1}^{3} A_i, \tag{16}$$

denotes an effective longitudinal stiffness, and

$$H = \frac{k_x + k_y}{2}, \tag{17}$$

represents the initial Gaussian curvature of the middle surface. Eq. (15) shows that n is not explicitly affected by the shear [22].

3. Equation of motion and boundary conditions

The equations of motion are derived by considering the free-body diagram of an infinitesimal shell element, loaded by the lateral forcing function $p(x, y; t)$. Thereby, in a common approximation, both, the longitudinal as well as the rotatory inertia are neglected, ${}_i\ddot{u}_j^{(0)} = 0$, ${}_i\ddot{\psi}_j^{(0)} = 0$, thus, limiting the analysis to the lower frequency band of structural dynamics. Conservation of momentum in z-direction and conservation of angular momentum with respect to the x- and y-coordinates give:

$$q_{x,x} + q_{y,y} + p + n(\Delta w - 2H) = \mu\ddot{w}, \tag{18}$$

$$m_{y,y} + m_{xy,x} - q_y = 0, \quad m_{x,x} + m_{xy,y} - q_x = 0. \tag{19}$$

Substitution of Eqs. (10) and (11) into Eqs. (18) and (19) and combination of Eqs. (18) and (19) after derivative with respect to x and y renders after some algebra the following equation of motion of the nonlinear shallow shell problem in terms of the lateral deflection w,

$$K\nabla^2\nabla^2 w + Ks_e n\left(\nabla^2\nabla^2 w - 2\nabla^2 H\right) - n\left(\nabla^2 w - 2H\right) - \mu K s_e \nabla^2\ddot{w} + \mu\ddot{w} = p - Ks_e\nabla^2 p. \tag{20}$$

Expression (20) may be understood as the equation of motion of a single-layer isotropic shear deformable shallow shell with mass per unit area μ, effective shear rigidity s_e, and flexural stiffness K. The effective properties are given by:

$$\mu = 2\rho_1 h_1 + \rho_2 h_2, \quad s_e = \frac{\gamma\chi}{K}, \quad K = \frac{2}{1-\nu}(2C_1 + C_2), \tag{21a}$$

$$\gamma = \frac{2}{1-\nu}\left[B_1 h_1\left(\frac{G_2}{G_1} - 1\right) + 2C_1\frac{G_2}{G_1} - C_2\right]. \tag{21b}$$

In Eq. (21a) ρ_1, ρ_2 denote the mass densities of the faces and the core, respectively.

The boundaries of the shallow shell are simply supported (i.e., the displacements are restrained and the bending moment is zero), and the individual in-plane cross-sectional rotations are restrained. These boundary conditions of the hard hinged type can be modeled in the form [19],

$$\Gamma: w = 0, \;\; {}_i\psi_s = 0, \;\; m_n = 0, \quad i = 1, 2, 3, \tag{22}$$

where n, s are local Cartesian coordinates at boundary Γ with normal n pointing outwards. Furthermore, conservation of momentum in z-direction at Γ for a differential shell element renders:

$$\Gamma: q_{n,n} + q_{s,s} + n\left(\nabla^2 w - 2H\right) + p = 0. \tag{23}$$

Considering only polygonal contours Γ (i.e. straight edges) $w = 0$ can be expressed by $w_{,s} = w_{,ss} = 0$, and ${}_i\psi_s = 0$ may be replaced by ${}_i\psi_{s,s} = 0$. Evaluating Eqs. (22) and (23) leads to two boundary conditions in w,

$$\Gamma : w = 0, \quad \nabla^2 w + s_e n\left(\nabla^2 w - 2H\right) = -s_e p. \tag{24}$$

According to Ref. [12,18] overall effective cross-sectional rotations ${}_e\psi_x$, ${}_e\psi_y$ (common to all layers) may be found by equating the overall shear forces of the current shell problem, Eq. (11), with the shear force of a corresponding single-layer shear deformable shallow shell [8],

$$q_j = \frac{1}{s_e}\left({}_e\psi_j + w_{,j}\right), \tag{25}$$

and subsequent decomposition as

$${}_e\psi_j = \frac{s_e}{\chi}\,{}_2\psi_j + \left(\frac{s_e}{\chi} - 1\right) w_{,j}, \quad j = x, y. \tag{26}$$

Eq. (26) are substituted into Eq. (10) and also the overall bending and twisting moments are obtained in analogy to a homogeneous shallow shell.

Utilizing ${}_e\psi_x$, ${}_e\psi_y$ the equation of motion (20) can be separated to form a set of three equations,

$$-\frac{1}{S_e}\left(\nabla^2 w + {}_e\psi_{x,x} + {}_e\psi_{y,y}\right) - n\left(\nabla^2 w - 2H\right) + \mu\ddot{w} = p - \frac{1}{S_e}, \tag{27a}$$

$$-K\left({}_e\psi_{j,jj} + \frac{1-\nu}{2}\,{}_e\psi_{j,kk} + \frac{1+\nu}{2}\,{}_e\psi_{k,jk}\right) - \frac{1}{s_e}\left({}_e\psi_j + w_j\right) = 0, \;\; j = x, k = y \quad \text{and} \quad k = x, \;\; j = y, \tag{27b}$$

and the boundary conditions (24) may be re-written as

$$\Gamma : w = 0, \; {}_e\psi_s = 0, \; {}_e\psi_{n,n} = 0. \tag{28}$$

It is noted that Eqs. (27) and (28) describe the higher-order problem of moderately large flexural vibrations of a shallow shell with straight edges on hard hinged immovable supports, which is modeled by piece-wise continuous in-plane displacement fields, in full analogy to the lower-order engineering theory of a corresponding isotropic single-layer shallow shell (with identical planform, initial curvature and boundary conditions). Hence, all solution techniques developed for homogenous shear deformable shallow shell become applicable to determine the kinematic variables w, ${}_e\psi_x$ and ${}_e\psi_y$ of the actual boundary value problem.

In a subsequent step the individual cross-sectional rotations of the core ${}_2\psi_x$, ${}_2\psi_y$ and of the faces ${}_1\psi_x$, ${}_1\psi_y$ are derived by decomposition of Eqs. (26) and (6), [12],

$${}_2\psi_j = \frac{\chi}{s_e}\,{}_e\psi_j - \left(1 - \frac{\chi}{s_e}\right) w_j, \;\; {}_1\psi_j = \frac{G_2}{G_i}\left({}_2\psi_j + w_{,j}\right) - w_{,j}, \quad i = 1, 3, \quad j = x, y. \tag{29}$$

4. Nonlinear steady-state response of layered shallow shells

In the following the dynamic response of rectangular shallow shells to time-harmonic excitation is examined. The shells of length a, width b and thickness h consist of three layers with layer to overall thickness ratios of $h_2/h = h_3/h = \frac{1}{3}$. The overall dimension is characterized by the aspect ratio $a/b = \frac{2}{3}$ and by the thickness to length ratios $h/a = \frac{1}{10}$ and $\frac{1}{20}$, respectively. The mechanical properties of the faces and the core are specified through the ratio $G_{1(3)}/G_2 = 20$. Poisson's ratio is selected to be uniform to all layers, $\nu = 0.3$. A shear coefficient of $\kappa^2 = 1$ is considered. The mean curvature of the middle surface follows a sine half-wave according to:

$$H = \frac{\hat{w}_0}{2}\left(\frac{\pi^2}{a^2} + \frac{\pi^2}{b^2}\right) \sin\frac{\pi x}{a} \sin\frac{\pi y}{b}, \tag{30}$$

where $\hat{w}_0$ denotes rise of the middle surface (the maximum initial displacement with respect to the base plane of the shell), which is varied within the scope of the subsequent studies. Note that the x and y coordinates point in the direction of length a and b, respectively, and their origin is in a corner of the shell.

For the solution of the actual boundary value problem represented by Eqs. (15), (27) and (28) the kinematic variables w, ${}_e\psi_x$ and ${}_e\psi_y$ are expanded into the ortho-normalized set of mode shapes $\Phi^{(mn)}$, ${}_x\psi^{(mn)}$ and ${}_y\psi^{(mn)}$,

$$w(x,y;t)=\sum_{m=1,n=1}^{\infty} Y_{mn}(t)\Phi^{(mn)}(x,y),\quad {}_e\psi_j(x,y;t)=\sum_{m=1,n=1}^{\infty} Y_{mn}(t)\,{}_j\Psi^{(mn)}(x,y),\quad j=x,y, \tag{31}$$

of the corresponding linearized shallow shell equations. For a rectangular shear deformable shallow shell the mode shapes are given by:

$$\Phi^{(mn)}(x,y)=A_{mn}\sin a_m x\sin b_n y,\quad n=1,\ldots,\infty,\quad m=1,\ldots,\infty, \tag{32a}$$

$${}_x\Psi^{(mn)}(x,y)=B_{mn}\cos a_m x\sin b_n y,\quad {}_y\Psi^{(mn)}(x,y)=C_{mn}\sin a_m x\cos b_n y, \tag{32b}$$

$$A_{mn}=\frac{2}{\sqrt{ab}},\quad B_{mn}=-\frac{A_{mn}a_m}{Ks_e\alpha_{mn}+1},\quad C_{mn}=-\frac{A_{mn}b_n}{Ks_e\alpha_{mn}+1},\quad a_m=\frac{m\pi}{a},b_n=\frac{n\pi}{b}. \tag{33}$$

Note that the mode shapes of the flat rectangular plate with equally shaped base plane and of the shell are the same, i.e. they are not affected by the Gaussian curvature H, which is proportional to the fundamental mode shape $\Phi^{(11)}$, see Eq. (30), Ref. [23] and Appendix A. Multiplication of the mode expanded equations with the srth mode shape for $sr=1\ldots\infty$ and subsequent integration about the planform of the shell leads under consideration of the orthogonality properties of the mode shapes to a coupled set of nonlinear ordinary differential equations for the modal coordinates Y_{mn},

$$\begin{aligned}&\ddot{Y}_{mn}+2\zeta_{mn}\omega_{mn}\dot{Y}_{mn}+\omega_{mn}^2Y_{mn}+\frac{D}{\Omega\mu}\alpha_{mn}\frac{\alpha_{11}}{A_{11}}\hat{w}_0Y_{mn}Y_{11}\\&+\frac{D}{2\Omega\mu}\left(\alpha_{mn}Y_{mn}\frac{\alpha_{11}}{A_{11}}\hat{w}_0\delta_{11}\right)\sum_{r,s=1}^{\infty}\alpha_{rs}Y_{rs}^2=\frac{1}{\mu}P_{mn},\quad n=1,\ldots,\infty,\quad m=1,\ldots,\infty.\end{aligned} \tag{34}$$

In Eq. (34) α_{mn} is the mnth Dirichlet Helmholtz eigenvalue of the corresponding rectangular membrane, see Refs. [16, p. 472],

$$\alpha_{mn}=a_m^2+b_n^2 \tag{35}$$

and ω_{mn} denotes the mnth natural circular frequency of the linearized shallow shell, see Ref. [23] and Appendix A,

$$\omega_{mn}=\sqrt{\frac{1}{\mu}\left[\frac{K\alpha_{mn}^2}{Ks_e\alpha_{mn}^2+1}+\frac{D\hat{w}_0^2\alpha_{11}^2}{\Omega A_{11}^2}\delta_{11}\right]}, \tag{36}$$

δ_{11} denotes the Kronecker delta ($=1$ for $nm=11$, otherwise $=0$), i.e. only the fundamental frequency is influenced by the mean curvature H. The mnth modal load coefficient is determined by

$$P_{mn}(t)=\int_{\Omega}\Phi_{mn}(x,y)p(x,y;t)\,\mathrm{d}\Omega. \tag{37}$$

In Eq. (34) structural damping has been introduced via modal damping coefficients ζ_{mn}. Incorporation of viscous damping in the response is another convenient feature of the modal approach to the nonlinear problem. In the subsequent computations all included damping coefficients are set equally to $\zeta_{mn}=0.05$.

Note that Eq. (34) contains nonlinear quadratic terms in the form ${Y_{rs}}^2$ with $r,s\neq m,n$. The mixed quadratic terms vanish because the mode shapes of the considered shells and the curvature of the middle surface are proportional. The nonlinear cubic terms of the (m,n)-oscillator are proportional to Y_{mn}. Non-proportional cubic terms do not occur in this equation because the mode shapes of the considered shells and the curvature of the middle surface are proportional, and the nonlinear behavior of the structures is described simplified by

means of Berger's theory (Eq. (15)). Compare with studies (Refs. [24,25]) devoted to homogeneous shell vibrations, where terms in form $Y_{pq}\ Y_{rs}$ and $Y_{pq}\ Y_{rs}\ Y_{tu}$ with $p, q, r, s, t, u \neq m, n$ are present in the mnth modal equation.

In particular, linear and nonlinear frequency response functions due to a uniformly distributed lateral load:

$$p(x, y; t) = p_0 \sin \upsilon t, \tag{38}$$

are derived by sweeping the excitation frequency υ. For the present study the load amplitude p_0 is presented in non-dimensional form according to:

$$p* = \frac{p_0 a^3}{K}. \tag{39}$$

For this non-dimensional representation of the lateral load it is assumed that the characteristic length of the shell is a. At time $t = 0$ the time-harmonic load is subjected to the shell and the nonlinear modal Eq. (34) are solved performing a time history analysis. Thereby, the infinitive series (31) are approximated by considering the first 4 symmetric modes. The corresponding mode shapes are shown in Fig. 3. Tentative calculations varying the number of modes have shown that this approximation is sufficient for prediction of the harmonic response of the considered structures. A discussion about the required number of modes is given by Alhazza [3]. After decay of the transient response the maximum of the steady-state response is recorded. It is assumed that the of the transient regime is reached when 8 consecutive maxima and minima of the dynamic response do not differ from each other more then 0.1%.

Fig. 4 shows non-dimensional amplitude functions of the lateral deflection at the center for thick shells (i.e., $h/a = 0.1$) with various radii of initial curvatures, which are characterized by the shell rise to thickness ratio $\hat{w}_0/h$. The corresponding non-dimensional load amplitude p^* is 1.0. The amplitude functions W_+ are normalized by means of the corresponding static central deflection w_{s+}, due to the static external pressure $p = p_0$; and the excitation frequency υ is related to the fundamental frequency ω_{11} of the corresponding linear plate with identical shape (i.e., $\hat{w}_0/h = 0$). Note that W_+ is the inward displacement amplitude (in direction of the center of curvature), which is different from the outward amplitude W_-. For the definition of W_+ and W_- see Fig. 5, where an example of a time history plot of the steady-state lateral displacement is shown. From Fig. 4 it can be seen that the plate exhibits a pronounced hard spring behavior. As the ratio $\hat{w}_0/h$ is increased the hard spring response diminishes and is reversed to a soft spring behavior. The shell with $\hat{w}_0/h = -0.50$ shows a soft spring response for small vibration amplitude, followed by a hard spring response as the

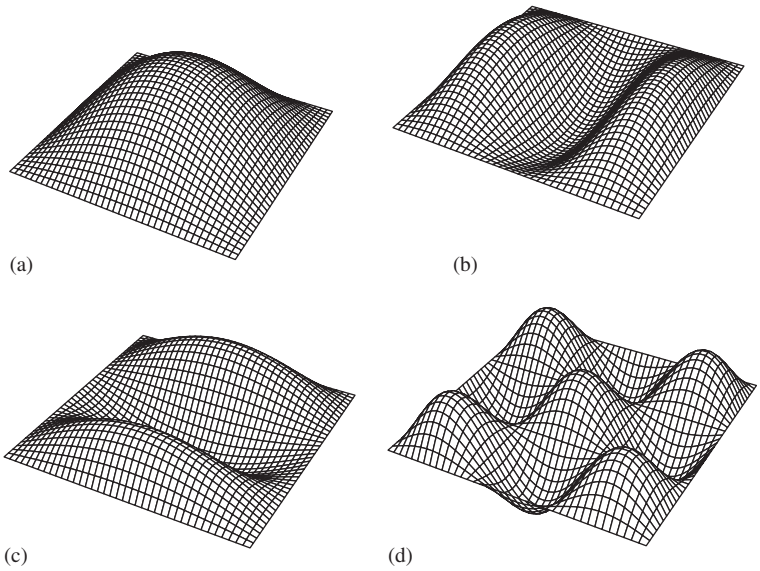

Fig. 3. Mode shapes retained in the analysis: (a) mode shape ϕ_{11}, (b) mode shape ϕ_{31}, (c) mode shape ϕ_{13}, (d) mode shape ϕ_{33}.

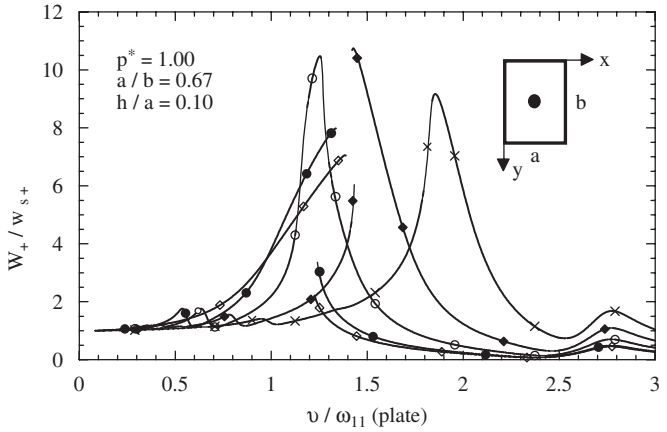

Fig. 4. Non-dimensional nonlinear amplitude functions of the lateral deflection at the center for different shell rise to thickness ratios $\hat{w}_0/h$: $\hat{w}_0/h = 0$, $\hat{w}_0/h = -0.25$, $\hat{w}_0/h = -0.50$, $\hat{w}_0/h = -0.75$, $\hat{w}_0/h = -1.00$. Stable branches of the response. Thick shell: $h/a = 0.10$.

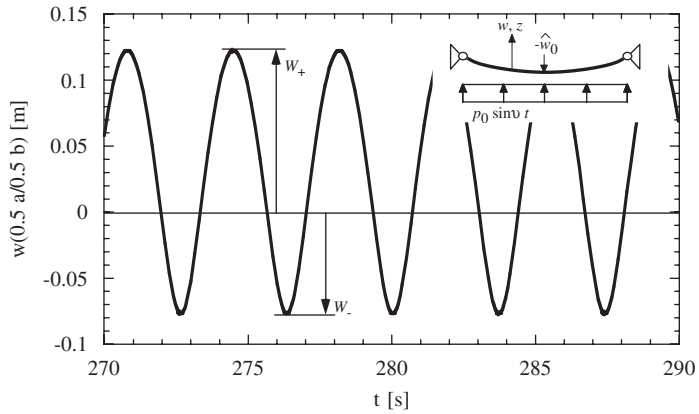

Fig. 5. Steady-state lateral displacement at the shell center. Definition of the amplitudes W_+ and W_-.

amplitude increases. This nonlinear behavior can be attributed to the fact that the initial stiffness of the shell is primarily membrane in nature, whereas for larger vibration amplitudes bending becomes dominant [9]. The bending deformation of the resonance curves leads for $\hat{w}_0/h = 0$, -0.25 and -0.75 to multivalued amplitudes and the entire solution splits into stable and unstable branches. At those points where the tangent is vertical the well-known jump phenomenon occurs. However, in Fig. 4 only the stable portions of the response are displayed (because the outcomes are derived by time history analyses). For all considered shell structures the influence of subharmonic resonance becomes visible by additional peaks at about half of the shell's linearized primary resonance frequency, i.e. the considered mode is excited by a signal of frequency close to half of its natural frequency.

In Fig. 6 normalized amplitude functions W_+ are depicted for a shell with $\hat{w}_0/h = -0.50$ in order to show the crossover from linear to nonlinear behavior with increasing magnitude of the applied load p^*. Note that W_+ due to $p^* = 1.00$ and 1.50 are both normalized with respect to w_{s+} due to $p^* = 1.00$. Note that the dynamic response close to the natural frequency ω_{13} with corresponding (second) symmetric mode shape is almost not affected by the nonlinear terms in the governing equations. The natural frequency ratio ω_{11}/ω_{13} of the considered shell is 0.476.

The convergence study shown in Fig. 7 demonstrates that a four mode presentation of the nonlinear dynamic response is sufficient to approximate the normalized amplitude functions W_+ at the center of the considered shallow shell examples.

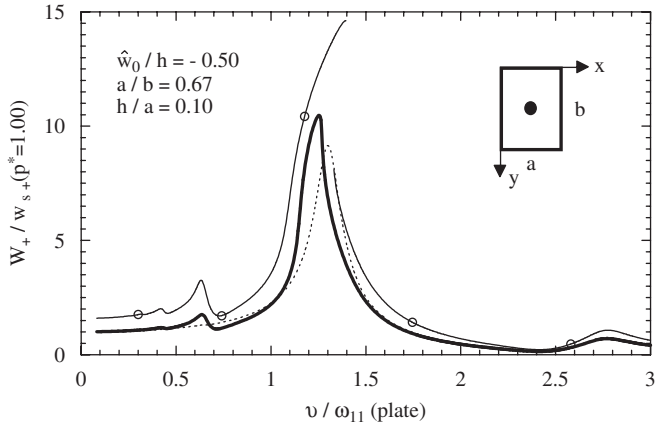

Fig. 6. Non-dimensional linear and nonlinear amplitude functions of the lateral deflection at the center for different non-dimensional loads p^*: ——— $p^* = 1.00$, —○— $p^* = 1.50$, ---------- linear. Stable branches of the response. Thick shell: $h/a = 0.10$.

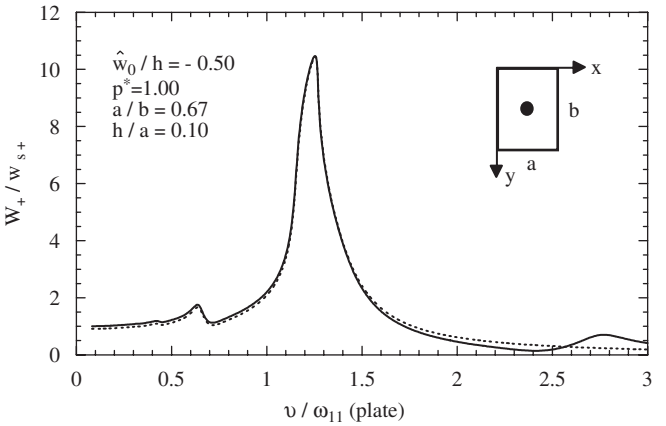

Fig. 7. Non-dimensional linear and nonlinear amplitude function of the lateral deflection at the center. $\hat{w}_0/h = -0.50$, $p^* = 1.00$: ——— response considering four modes, ---------- single mode approximation. Thick shell: $h/a = 0.10$.

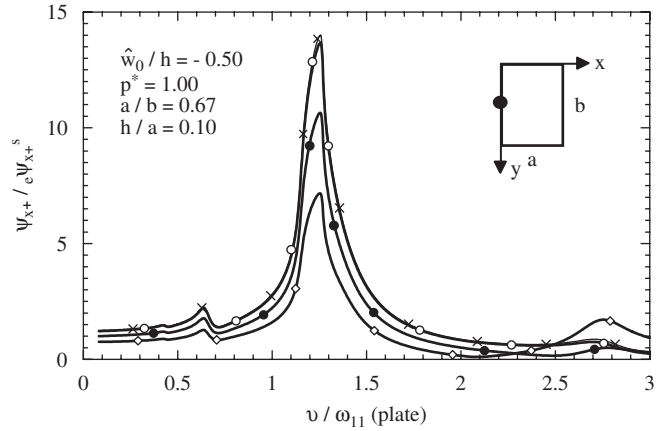

Fig. 8. Non-dimensional nonlinear amplitude functions of the layerwise and effective cross-sectional rotations in x-direction and of the derivation of the deflection with respect to x at ($x/y = 0/0.5$ b). $\hat{w}_0/h = -0.50$, $p^* = 1.00$: —○— ${}_1\Psi_{x+}$, —◇— ${}_2\Psi_{x+}$, —●— ${}_e\Psi_{x+}$, —×— $W_{,x+}$. Thick shell: $h/a = 0.10$.

Fig. 8 presents inward amplitude response functions of the individual cross-sectional rotations ${}_1\psi_x$ and ${}_2\psi_x$, the effective cross-sectional rotation ${}_e\psi_x$ and the derivative of the deflection with respect to x, $w_{,x}$, at point $(x/y = 0/0.5\ b)$ for the shell of same geometry. All individual rotation amplitude curves are normalized by means of the corresponding effective cross-sectional rotation ${}_e\psi^S_{x+}$ due to the static external pressure $p = p_0$. A non-dimensional load amplitude of $p^* = 1$ is considered. It can be seen that the cross-sectional rotations of the core and the faces do not coincide. In the primary resonance domain the amplitudes ${}_1\Psi_{x+}$ of the face response are larger than those of the core (${}_2\Psi_{x+}$), in the vicinity of the second excited mode ${}_2\Psi_{x+}$ exceeds ${}_1\Psi_{x+}$. The amplitude response ${}_1\Psi_{x+}$ is slightly overestimated by $W_{,x+}$ at the primary resonance frequency, otherwise the corresponding graphs are identical. Fig. 9 depicts amplitude response functions of the cross-sectional rotations ${}_1\psi_x$, ${}_2\psi_y$, ${}_e\psi_y$ as well as of $w_{,y}$ at point $(x/y = 0.5\ a/0)$, and they are related to the effective cross-sectional rotation ${}_e\psi^s_{y+}$ due to the static external pressure $p = p_0$. It is interesting to note that for this point the resonance curves of the faces exhibit larger magnitudes than those of the faces in the whole frequency range, which is a contradiction to the results of Fig. 8. From Figs. 8 and 9 it can be concluded that a layerwise description of the kinematic variables is essential to predict the behavior of the considered shallow shell.

The corresponding comparison between the inward and the outward vibration amplitudes is shown in Figs. 10–12. It is remarkable that the inward response amplitudes $W_{,x+}$, ${}_1\Psi_{x+}$, ${}_2\Psi_{x+}$ exceed in magnitude the

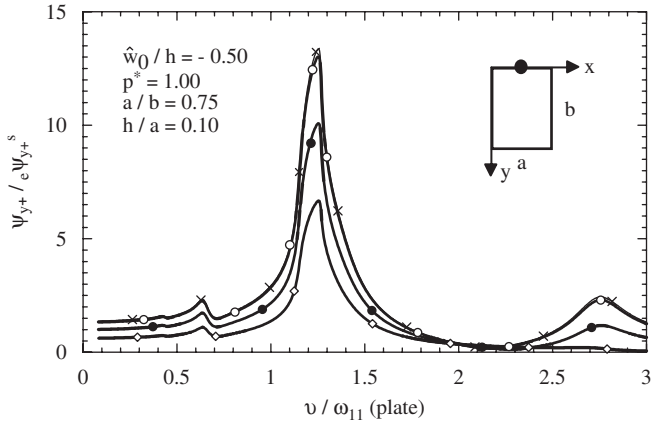

Fig. 9. Non-dimensional nonlinear amplitude functions of the layerwise and effective cross-sectional rotations in y-direction and of the derivation of the deflection with respect to y at $(x/y = 0.5\ a/0)$. $\hat{w}_0/h = -0.50$, $p^* = 1.00$: ——○—— ${}_1\Psi_{y+}$, ——◇—— ${}_2\Psi_{y+}$, ——●—— ${}_e\Psi_{y+}$, ——×—— $W_{,y+}$. Thick shell: $h/a = 0.10$.

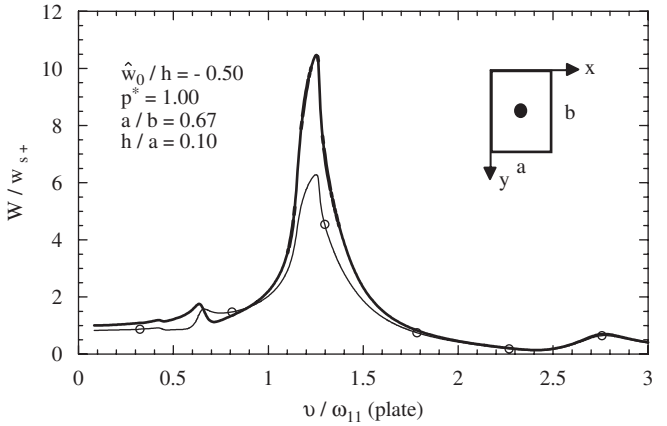

Fig. 10. Non-dimensional nonlinear amplitude functions of the lateral deflection at the center. ——— W_+: inward displacement amplitude; ——○—— W_-: outward displacement amplitude. Thick shell: $h/a = 0.10$.

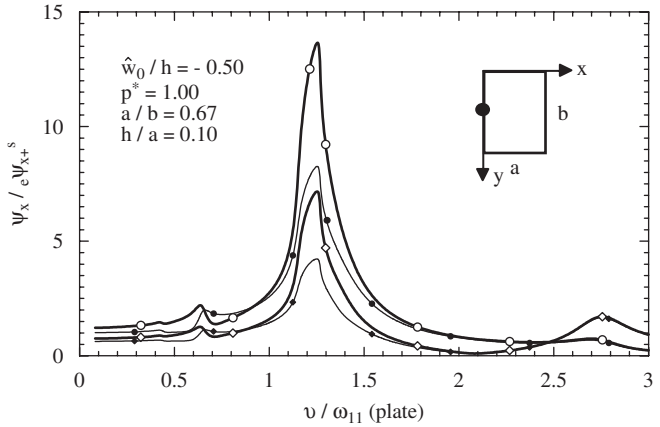

Fig. 11. Non-dimensional nonlinear amplitude functions of the layerwise cross-sectional rotations in x-direction at ($x/y = 0/0.5\ b$). Inward and outward amplitudes: $_1\Psi_{x+}$, $_1\Psi_{x-}$, $_2\Psi_{x+}$, $_2\Psi_{x-}$. Thick shell: $h/a = 0.10$.

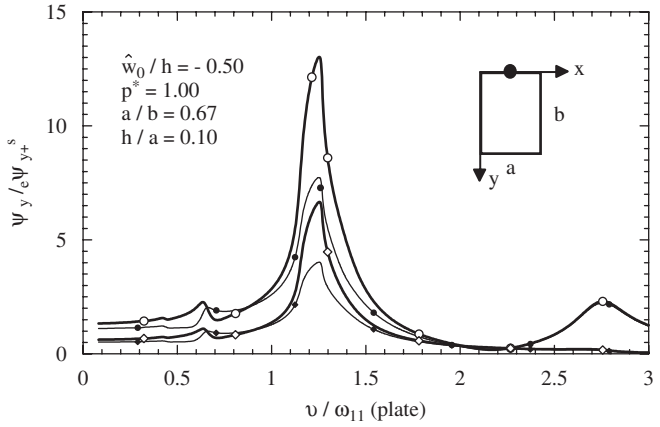

Fig. 12. Non-dimensional nonlinear amplitude functions of the layerwise cross-sectional rotations in y-direction at ($x/y = 0.5\ a/0$). Inward and outward amplitudes: $_1\Psi_{y+}$, $_1\Psi_{y-}$, $_2\Psi_{y+}$, $_2\Psi_{y-}$. Thick shell: $h/a = 0.10$.

outward displacements $W_{,x-}$, $_1\Psi_{x-}$, $_2\Psi_{x-}$ in the quasistatic and in the primary resonance domain. At higher frequencies the quantities are of the same magnitude, because the influence of the nonlinearities is diminishing.

Subsequently, a thin shallow shell with a thickness to length ratio $h/a = 0.05$ and a rise of $\hat{w}_0/h = -0.50$ is considered. In Fig. 13 the normalized amplitude functions W_+/w_{s+} of the lateral deflection at the shell center are presented for the magnitudes of the applied load p^* of 1.00 and 1.50. Fig. 14 shows normalized amplitude functions of the individual cross-sectional rotations $_1\psi_x$ and $_2\psi_x$, the effective cross-sectional rotation $_e\psi_x$ and the derivative of the deflection with respect to x, $w_{,x}$, at point ($x/y = 0/0.5\ b$) for $p^* = 1.00$. It can be seen that for this thin shell the cross-sectional rotations of the faces and of the core are almost identical in the quasi-static frequency range, i.e. the in-plane displacements of the structure could be described by means of a single cross-sectional rotation common to all layers. With increasing excitation frequency a difference between the individual cross-sectional rotations becomes apparent, which is significant at $\upsilon/\omega_{11}(\text{plate}) = 3.2$. From this result it can be concluded that the importance of a layerwise description of the displacement field is not only a function of geometry and material parameters but also of the considered frequency range.

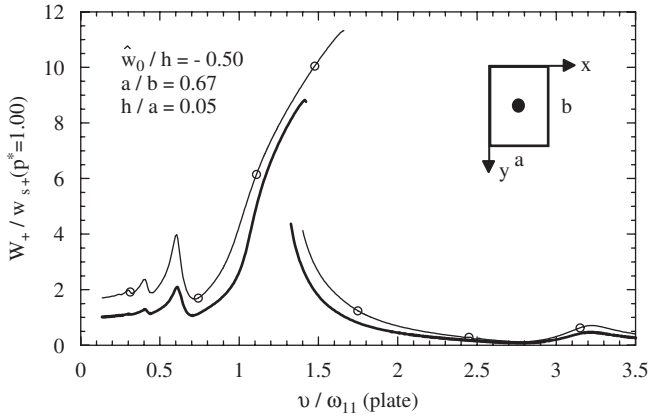

Fig. 13. Non-dimensional linear and nonlinear amplitude functions of the lateral deflection at the center for different non-dimensional loads p^*: ——— $p^* = 1.00$, —o— $p^* = 1.50$. Stable branches of the response. Thin shell: $h/a = 0.05$.

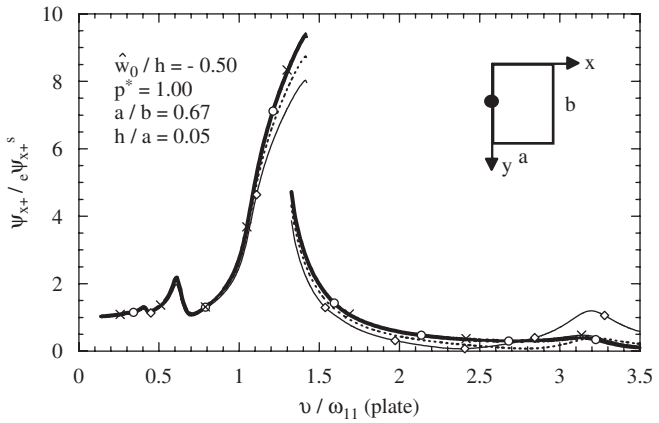

Fig. 14. Non-dimensional nonlinear amplitude functions of the layerwise and effective cross-sectional rotations in x-direction and of the derivation of the deflection with respect to x at ($x/y = 0/0.5$ b). $\hat{w}_0/h = -0.50$, $p^* = 1.00$: —o— ${}_1\Psi_{x+}$, —◇— ${}_2\Psi_{x+}$, --------- ${}_e\Psi_{x+}$, —×— $W_{,x+}$. Thick shell: $h/a = 0.05$.

5. Conclusions

Based upon a layerwise first-order theory nonlinear equations of motions for moderately large amplitude vibrations of composite doubly curved shallow open shells with polygonal planform are derived. The three layers of the considered shell structures are symmetrically arranged about the middle surface, and may possess extremely different shear flexibility. The displacements of the hard hinged supported edges are restrained in any direction, and thus, geometric nonlinearities are accounted for according to Berger's approximation. Amplitude frequency response functions of rectangular shallow shells with a Gaussian curvature affine to the linearized fundamental mode shape are found by a modal projection of the nonlinear response variables according to the corresponding linearized mode shapes. Depending on the shell rise the considered structures exhibit hardening or softening type of response behavior, or, depending on the initial curvature, a combination of both. From the results it can be concluded that for thick shells a layerwise description of the kinematic variables is essential to predict the in-plane displacement response with sufficient accuracy. For thin shell a single cross-sectional rotation may describe with sufficient accuracy the displacement field in the low frequency range.

Appendix A

In this appendix the main results of Ref. [23] are summarized, where free vibrations of shear deformable shallow shells with polygonal planform are studied. Linearization of Eq. (20) leads to the differential equation of motion for free small amplitude vibrations w_l of the shallow shell,

$$K\Delta\Delta w_l - 2Ks_e n_l \Delta H + 2n_l H - \mu K s_e \Delta\ddot{w}_l + \mu\ddot{w}_l = 0, \tag{A.1}$$

$$n_l = \frac{2D}{\Omega}\int_\Omega w_l H \,\mathrm{d}\Omega, \quad H(x,y) = -\frac{1}{2}\Delta\hat{w}(x,y), \tag{A.2}$$

with the precurvature of the shell $\hat{w}$. The lateral deflection w and the Gaussian curvature H are expanded in a series of functions, which satisfy the boundary conditions. This is provided by the mode shapes of the corresponding plate (i.e., same plane form and boundary conditions as the shallow shell) $\Phi^{(mn)}(x, y)$; for the considered shell problem see Eq. (32a). Thus, w and H may be expressed by

$$w_l(x,y;t) = \sum_{m=1,n=1}^{\infty} Y^l_{mn}(t)\Phi^{(mn)}(x,y), \quad H = -\frac{1}{2}\sum_{m=1,n=1}^{\infty}\frac{\gamma_{mn}}{A_{mn}}\Delta\Phi^{(mn)}(x,y). \tag{A.3}$$

The coefficients γ_{mn} are defined by the initial curvature, whereas the time-dependent coordinates $Y^l_{mn}(t)$ are the new unknown in the differential equation. Inserting Eq. (A.3) into Eq. (A.1), multiplication by $\Phi^{(rs)}$ for $rs = 1, \ldots, \infty$ and integration over the plane form leads due to the orthogonality of $\Phi^{(rs)}$ to a coupled set of ordinary differential equations for $Y^l_{mn}(t)$,

$$\ddot{Y}^l_{mn} + \sum_{i=1,j=1}^{\infty} a_{mnij}\, Y^l_{ij} = 0, \tag{A.4}$$

$$a_{mnij} = \frac{1}{\mu}\left[\frac{K\alpha^2_{mn}\delta_{mnij}}{Ks_e\alpha_{mn}+1} + \frac{D\gamma_{ij}\alpha_{ij}\gamma_{mn}\alpha_{mn}}{\Omega A^2_{ij}}\right], \quad \gamma_{mn} = A_{mn}\int_\Omega \hat{w}\Phi^{(mn)}\,\mathrm{d}\Omega, \tag{A.5}$$

where δ_{mnij} denotes the Kronecker delta ($= 1$ for $nm = ij$, otherwise $= 0$). From this set of equations the natural frequencies of the shallow shell are computed. It can be seen that the coupling terms a_{mnij} are tied to the existence of γ_{mn}. When the Gaussian curvature is affine to the rsth shape function $\Phi^{(rs)}$ the linearized curvature of Eq. (A.3) is reduced to $H = -\gamma_{rs}\Delta\Phi^{(rs)}/2$, where γ_{rs} determines the maximum rise of the shell. All other coefficients γ_{mn} vanish: $\gamma_{mn} = 0$ ($mn \neq rs$). Thus, the coefficients a_{mnij} are simplified and all coupling terms in Eq. (A.4) are eliminated. Then, the natural frequencies of the shallow shell are derived as,

$$\omega_{mn} = \sqrt{\frac{1}{\mu}\left[\frac{K\alpha^2_{mn}}{Ks_e\alpha_{mn}+1} + \frac{D\gamma^2_{rs}\alpha^2_{rs}}{\Omega A^2_{rs}}\delta_{mnrs}\right]}. \tag{A.6}$$

From this equation it can be observed that the frequency increase caused by the curvature is independent of the shear stiffness. In Eq. (A.6) $\gamma_{mn} = 0$ ($mn \neq rs$), and thus only the natural frequency ω_{rs} is affected by the initial curvature, whereas all other natural frequencies coincide with the natural frequencies of the corresponding plate.

References

[1] M.S. Qatu, Recent research advances in the dynamic behavior of shells: 1989–2000, part 1: laminated composite shells, *Applied Mechanics Reviews* 55 (4) (2002) 325–349.

[2] M.S. Qatu, *Vibrations of Laminated Shells and Plates*, Academic Press, UK, 2004.

[3] K.A. Alhazza, A.A. Alhazza, A review of vibrations of plates and shells, *The Shock and Vibration Digest* 36 (5) (2004) 377–395.

[4] K.M. Liew, C.W. Lim, S. Kitipornchai, Vibration of shallow shells: a review with bibliography, *Applied Mechanics Reviews* 50 (8) (1997) 431–444.

[5] M.S. Qatu, A.W. Leissa, Free vibrations of completely free doubly curved laminated composite shallow shells, *Journal of Sound and Vibration* 151 (1991) 9–29.

[6] M. Touratier, A refined theory of laminated shallow shells, *International Journal of Solids and Structures* 29 (1992) 1401–1415.
[7] Y.M. Fu, C.Y. Chia, Non-linear vibration and postbuckling of generally laminated circular cylindrical thick shells with non-uniform boundary conditions, *International Journal of Non-Linear Mechanics* 28 (1993) 313–327.
[8] R. Heuer, Large flexural vibrations of thermally stressed layered shallow shells, *Nonlinear Dynamics* 5 (1994) 25–38.
[9] Y. Kobayashi, A.W. Leissa, Large amplitude free vibration of thick shallow shells supported by shear diaphragms, *International Journal of Non-Linear Mechanics* 30 (1995) 57–66.
[10] J. Wang, K. Schweizerhof, Boundary-domain element method for free vibration of moderately thick laminated orthotropic shallow shells, *International Journal of Solids and Structures* 33 (1996) 11–18.
[11] Ku Shin Dong, Large amplitude free vibration behavior of doubly curved shallow open shells with simply-supported edges, *Computers and Structures* 62 (1997) 35–49.
[12] C. Adam, Moderately large flexural vibrations of composite plates with thick layers, *International Journal of Solids and Structures* 40 (2003) 4153–4166.
[13] H.M. Berger, A new approach to the analysis of large deflection of plates, *Journal of Applied Mechanics* 22 (1995) 465–472.
[14] T. von Kármán, H.S. Tsien, The buckling of cylindrical shells under axial compression, *Journal of Aeronautical Sciences* 8 (1941) 303–312.
[15] Y.-Y. Yu, *Vibrations of Elastic Plates*, Springer, New York, 1995.
[16] F. Ziegler, *Mechanics of Solids and Fluids*, second ed., Springer, New York, 1998.
[17] M.-J. Yan, E.H. Dowell, Governing equations for vibrating constrained-layer damping sandwich plates and beams, *Journal of Applied Mechanics* 39 (1972) 1041–1046.
[18] R. Heuer, Static and dynamic analysis of transversely isotropic, moderately thick sandwich beams by analogy, *Acta Mechanica* 91 (1992) 1–9.
[19] C. Adam, Dynamic analysis of isotropic composite plates using a layerwise theory, *Composite Structures* 51 (2001) 427–437.
[20] W.A. Nash, J.R. Modeer, Certain approximate analyses of the nonlinear behavior of plates and shallow shells, in: W.T. Koiter (Ed.), *Proceedings of the IUTAM-Symposium on the Theory of Thin Elastic Shells, Delft, 1959*, North-Holland Publishing Company, Amsterdam, 1960, pp. 331–354.
[21] R. Heuer, F. Ziegler, Thermoelastic stability of layered shallow shells, *International Journal of Solids and Structures* 41 (2004) 2111–2120.
[22] C.-I. Wu, J.R. Vinson, Influences of large amplitudes, transverse shear deformation, and rotatory inertia on lateral vibrations of transversely isotropic plates, *Journal of Applied Mechanics* 36 (1969) 254–260.
[23] M. Hochrainer, U. Pichler, H. Irschik, Membrananalogie für Eigenfrequenzen flacher Schalen, *Zeitschrift für Angewandte Mathematik und Mechanik* 79 (S2) (1999) S409–S410 (in German).
[24] K.A. Alhazza, Nonlinear Vibrations of Doubly Curved Cross-ply Shallow Shells. PhD Thesis, Virginia Polytechnic Institute and State University, 2002.
[25] O. Thomas, C. Touzé, A. Chaigne, Non-linear vibrations of free-edge thin spherical shells: modal interaction rules and 1:1:2 internal resonance, *International Journal of Solids and Structures* 42 (11) (2005) 3339–3373.